# Overcoming photocatalytic hydrogen atom transfer (HAT) limitations via formyl-group directed C–H cleavage

Elena Cassera,[a,‡] Vittoria Martini,[b,‡] Serena Abrami,[b] Nicola Della Ca',[b] Davide Ravelli,[a] Maurizio Fagnoni,[a,*] Luca Capaldo [b,*]

[a] PhotoGreen Lab, Department of Chemistry, University of Pavia, viale Taramelli 12, 27100 Pavia, Italy.
[b] SynCat Lab, Department of Chemistry, Life Sciences and Environmental Sustainability, University of Parma, Parco Area delle Scienze 17/A, 43124 Parma, Italy.
E-mail: luca.capaldo@unipr.it; maurizio.fagnoni@unipv.it

[‡] These authors contributed equally to this work.

**ABSTRACT:** Photocatalyzed Hydrogen-Atom Transfer (HAT) is now an established methodology in the synthesis of pharmaceuticals and agrochemicals, as well as in the development of late-stage functionalization campaigns. Yet, the realization of the full potential of this manifold is held back by intrinsic challenges that still demand meticulous exploration and resolution, such as lack of regioselectivity and inefficiency. Herein, we propose the HAcTive strategy to address these longstanding challenges. The fast HAT from aldehydes formyl group and ensuing α-fragmentation of the photogenerated acyl radical (i.e. decarbonylation) is exploited to boost efficiency, steer regioselectivity and enable reactivity in HAT-based methodologies. We validated this concept in several decarbonylative C–C bond formation protocols. In-depth mechanistic investigation based on Laser-Flash Photolysis and Density Functional Theory highlight the crucial role of kinetic factors to control the observed chemistry.

## INTRODUCTION

In the new century, there has been a surge in synthetic methods based on the generation of radicals, especially carbon-centered radicals. Photocatalyzed hydrogen atom transfer (HAT) has attracted substantial attention from synthesis practitioners to access these intermediates, often being hailed as the holy grail of synthetic methodology (Figure 1A).[1-5] In fact, a suited photocatalyst absorbs a photon and cleaves homolytically an *aliphatic* C–H bond from an H-atom donor to produce the desired organoradical.

Although riveting, the realization of the full potential of this manifold is accompanied by challenges that still demand meticulous exploration and resolution (Figure 1B). Foremost among these challenges is

the issue of *regioselectivity*. In fact, C–H bonds are omnipresent in organic molecules, which calls for the development of tactics to achieve regioselectivity in the C–H cleavage step. This selectivity can be somewhat adjusted by mastering the complex interplay between substrate, photocatalyst and medium characteristics,[6-12] but full control still remains out of reach. Another major limitation for the wide adoption of photocatalyzed HAT is represented by *inefficiency*. To cope with this, H-atom donors are typically used in superstoichiometric amounts, which is paradoxical given the intrinsic atom-economy of HAT. While this might not be a significant obstacle when working with readily accessible substrates (e.g. tetrahydrofuran or cyclohexane), it is a considerable limitation for late-stage functionalization endeavours.[13] Indeed, in these instances, employing multiple equivalents of the H-atom donors may be unfeasible due to restricted availability and substantial cost of the starting materials.[5]

Determined to address the two limitations outlined above, we were inspired by photoredox catalysis.[14-18] Here, a photocatalyst engages with the substrate via a photoinduced single-electron transfer (SET) step instead of hydrogen atom transfer (HAT). To promote SET, a so-called *redox auxiliary group* is often introduced in the substrate to match its redox potential with that of the excited state of the photocatalyst. Upon successful electron transfer, mesolytic cleavage of the auxiliary group occurs to reveal the desired carbon-centered radical. Overall, the use of redox auxiliary groups often allows to avoid using the radical progenitor in excess and ensures site-selectivity in the formation of the radical. We became intrigued in extrapolating this concept to the field of photocatalyzed HAT by taking advantage of a Traceless Activating Group (TAG, Figure 1C). This group should be activated via HAT and react faster than most typical aliphatic C–H bonds found in organic molecules. This ensures that the H-donor can be used in stoichiometric amount (1 equivalent). Moreover, the radical generated via HAT from the TAG should undergo prompt fragmentation to reliably reveal the desired organoradical with minimum impact on atom-economy of the process. Finally, the TAG is a functional group that is commonly found in organic molecules (or easily installed), therefore granting access to structurally diverse alkyl radicals (Figure 1C). In view of the above, we identified the formyl group of aldehydes as the ideal TAG for photocatalyzed HAT.[19]

In fact, besides C($sp^3$)–H bonds, photocatalyzed HAT can be exploited for the activation of aldehydic formyl C($sp^2$)–H bonds to yield acyl radicals as well.[20-26] The latter intermediates are directly exploited for the synthesis of unsymmetrical ketones,[21,27-31] however competitive decarbonylation to unveil alkyl radicals was in some cases documented. For example, Fagnoni and co-workers observed competitive decarbonylation when attempting acylation of electrophilic olefins.[25] A few years later, Orfanopoulos observed a similar phenomenon while developing a procedure for the acylation of [60]fullerene.[26] More recently, Wu and co-workers showed that α-alkoxyaldehydes and pivalaldehyde undergo complete decarbonylation in a Co-based dehydrogenative strategy.[20] Although in those instances the decarbonylation pathway was identified as a selectivity issue, which was addressed by decreasing the

reaction temperature,[25,26] we reasoned that this pathway could be turned into a new strategy to tackle the abovementioned limitations of HAT photocatalysis.

Herein, we report the successful implementation of this concept, which we name HAcTive (Figure 1D), for C–C bond forming reactions. First, we demonstrate that this strategy enables more practical conditions for photocatalyzed HAT, by lowering the excess of H-donor needed to achieve efficient transformations. Second, we show that the introduction of the TAG improves selectivity of the overall process when the corresponding TAG-free substrate undergoes decomposition. Third, we demonstrate that it can be used to redirect regioselectivity in the hydrogen abstraction step, thus unlocking new opportunities in photocatalyzed synthesis. Moreover, as a testament of the potential of the HAcTive strategy, we developed a protocol for the formal synthesis of a wide range of Non-Proteinogenic Amino Acids (NPAAs) by exploiting the Garner's aldehyde as the model substrate. Finally, the working principles of a TAG have been uncovered through a combination of experimental, spectroscopic and computational studies.

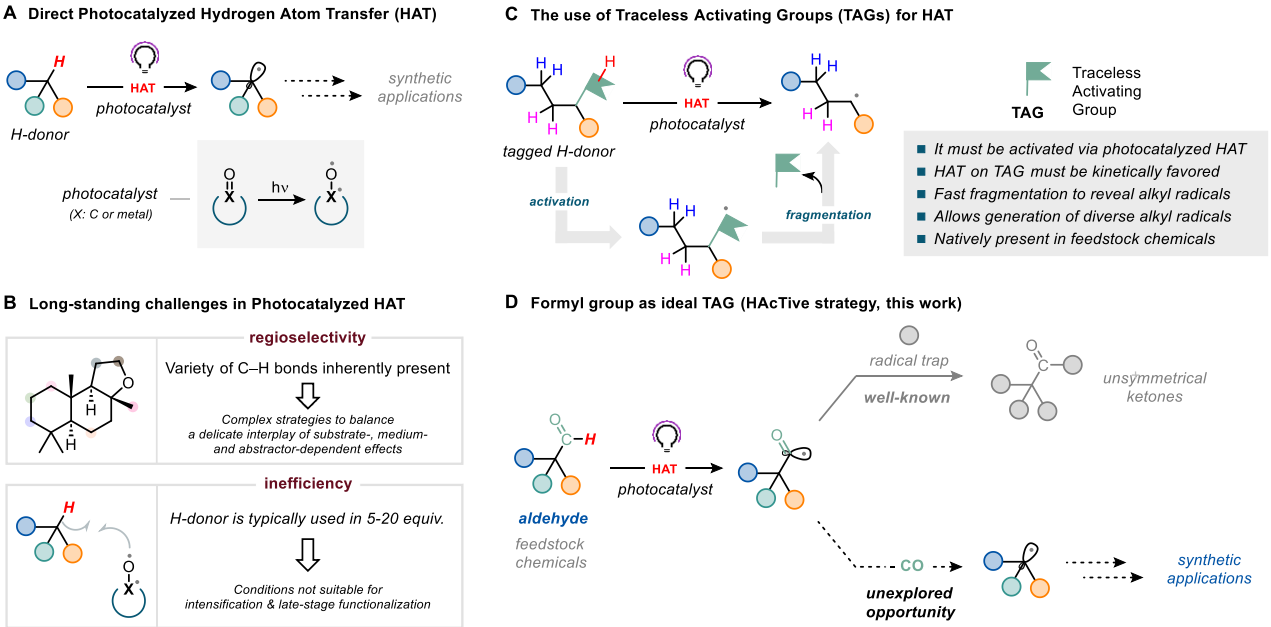


***Figure 1*** – A) Direct Photocatalyzed Hydrogen Atom Transfer (HAT). B) Regioselectivity and efficiency are long-standing challenges, still frustrating the wide adoption of HAT for process chemistry and late-stage functionalization campaigns. C) The concept of Traceless Activating Groups (TAGs) for photocatalyzed HAT. D) The HAcTive strategy.

## Results and Discussion

We started validating our concept by comparing the reactivity of methyl *tert*-butyl ether (**S1**) and alkoxyaldehyde **1a** in a Giese-type radical hydroalkylation reaction. The decatungstate anion (4 mol% as tetrabutylammonium salt, TBADT) was chosen as the photocatalyst to trigger the HAT step.[32-34] When the reactions were performed in the presence of 2-vinylpyridine as the SOMOphile under irradiation at

390 nm for 16 h, product **3** was detected (Figure 2A). As anticipated, **3** was formed only in trace amounts when 1.2 or 2 equivalents of **S1** were used. Interestingly, even with 5 equivalents of the H-donor, the yield did not exceed 30%, in spite of the total consumption of 2-vinylpyridine (Figure 2A). When replacing **S1** with the corresponding *tagged* H-donor **1a**, the advantage of the HAcTive strategy was immediately evident. Indeed, compound **3** was formed in good yield (79%) without the need for a large excess of the H-donor (1.2 equiv., Figure 2A). Interestingly, no competitive formation of the corresponding undesired acylated product was detected by GC-MS analysis and 2-vinylpyridine was completely consumed at the end of the reaction. This approach was verified across different classes of electrophilic olefins, including unsaturated esters (compounds **4** and **5**), nitriles (**6-8**), sulfones (**9**) and ketones (**10**), reliably delivering the expected Giese adducts in yields (Figure 2A). These results clearly show that the HAcTive strategy enables more practical conditions for photocatalyzed HAT.

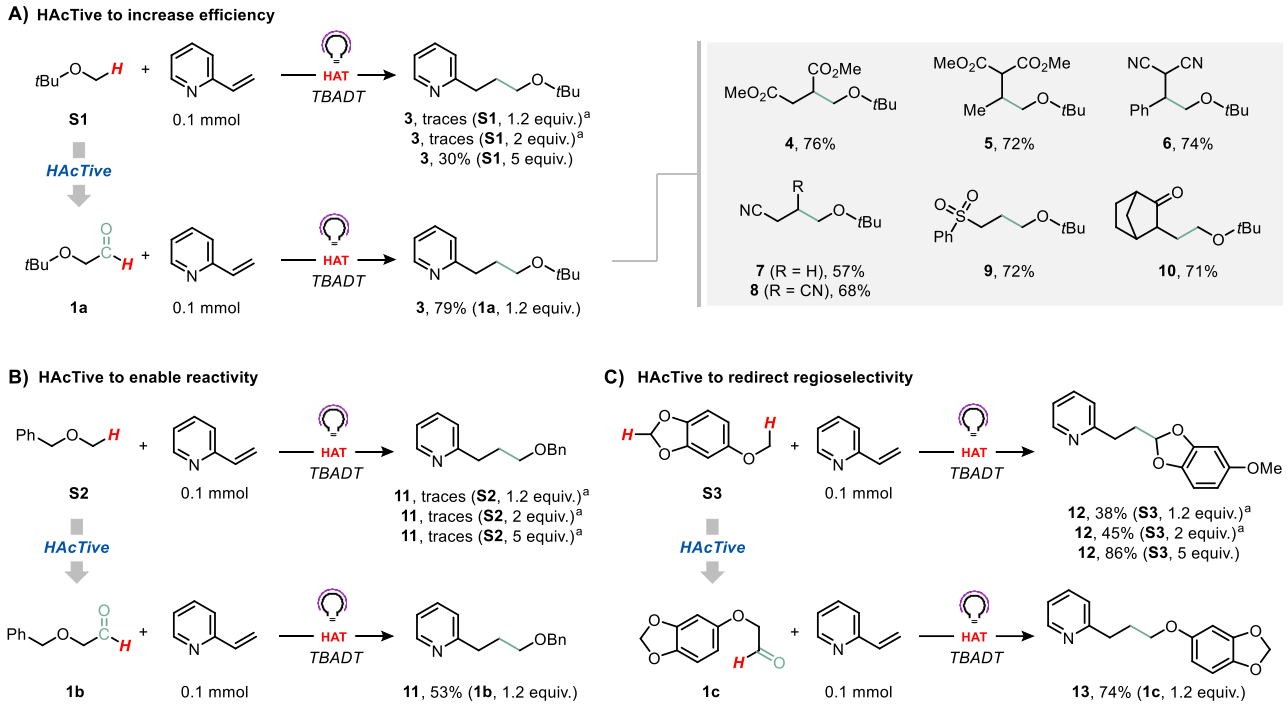


***Figure 2*** – Validation of the HAcTive strategy in a Giese-type radical hydroalkylation reaction to: A) increase reaction efficiency, B) enable reactivity for recalcitrant substrates and C) steer regioselectivity. Reaction conditions: H-donor (1.2-5 equiv.), 2-vinylpyridine (0.1 mmol) and TBADT (4 mol%) in $CH_3CN$ (0.1 M). The reaction mixture was bubbled with $N_2$ (1 min) before irradiation at 390 nm for 16 h. [a] Incomplete conversion of 2-vinylpyridine was observed.

On a different note, benzyl methyl ether (**S2**) is a poor substrate for the Giese reaction, most likely because of the competition between the two α-to-O positions for the HAT step (Figure 2B). In fact, a complex mixture resulted from the irradiation and the desired product **11** was detected only in traces, regardless of the amount of **S2** used (up to 5 equiv.). The outcome was completely different, however, when **1b** was used in the role of H-donor: compound **11** was isolated in a satisfying yield as the sole product in 53% yield (Figure 2B). Hence, in this case, the HAcTive strategy successfully revived a reaction that would otherwise be hindered by competing reaction pathways.

Next, we set off to probe the validity of our approach to steer regioselectivity in photocatalyzed HAT (Figure 2C). Thus, when sesamol methyl ether (**S3**) was used as the H-donor in our radical hydroalkylation conditions, product **12** was obtained in decent yields (38% with 1.2 equiv. of **S3**) with complete selectivity for the functionalization of the acetalic methylene site. The product deriving from the hydrogen abstraction on the methyl group was not observed. Higher concentrations of the H-donor improved the yield but left the regioselectivity unaltered. Impressively, when the *tagged* H-donor **1c** was adopted in only 1.2 equivalents, the regioselectivity was completely diverted and compound **13** was formed instead. In this case, product **12** was not observed (Figure 2C). Additional experiments on aldehydes **1f**-**1i** proving the generality of the HAcTive strategy are reported in Section 7 of the Supporting Information.

Motivated by the significant impact of the TAG, we started investigating whether the aforementioned effects could be integrated to design novel synthetic platforms for decarbonylative C–C bond formation. Inspired by recent work from Baran,[35] we opted to apply the HAcTive strategy to achieve the selective functionalization of the 2,2-dimethyl-oxazolidine ring (**S4**, Figure 3) as a convenient and atom-economical access point to 1,2-aminoalcohols. In fact, the oxazolidine ring contains two methylene groups — the α-to-N and α-to-O positions — that compete for functionalization via photocatalyzed HAT.

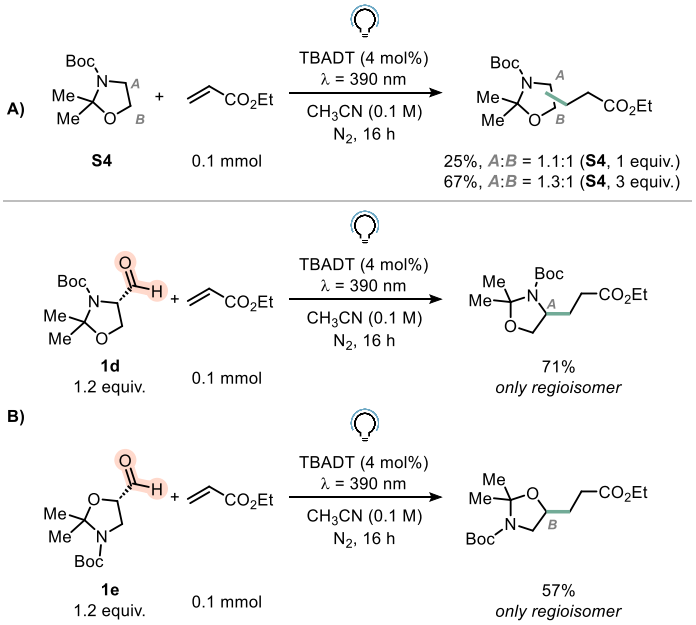


***Figure 3.*** A) The functionalization of oxazolidine **S4** via Giese-type radical addition leads to a mixture of regioisomers in low yield. B) The use of a TAG improves efficiency and selectivity. $^1$H-NMR yields are shown (internal standard: $CH_2Br_2$).

As the Bond Dissociation Energies of α-to-N and α-to-O C–H bonds are nearly identical (92[36] vs 90[37] kcal·mol$^{-1}$ for tetrahydrofuran and pyrrolidine, respectively), this issue cannot be effectively addressed on thermodynamic grounds. The Garner's aldehyde (**1d**) is a *tagged* surrogate for **S4** and it has attracted significant interest as a chiral intermediate for the enantioselective synthesis of amino alcohols.[38] It is

commercially available and can be synthesized efficiently on a large scale (see section 4.2 in the Supporting Information).[39] We hypothesized that the formyl group could function as an antenna for a *fast* HAT step, delivering an acyl radical. Ensuing decarbonylation would deliver a stabilized α-aminoalkyl radical. Overall, the formyl group would serve as a TAG to outcompete H-abstraction from the α-to-O site.

These hypotheses were fully confirmed by our experimental work (Figure 3). In fact, under the reaction conditions outlined in Figure 2, the adoption of oxazolidine **S4** (1.2 equiv.) as the hydrogen donor and ethyl acrylate as the radical trap led to functionalization at both the α-to-N and α-to-O positions in a 1.1:1 ratio and with a modest overall yield of 25% (Figure 3A). In sharp contrast, using **1d** (1.2 equiv.) as the hydrogen donor significantly improved the reaction, resulting in selective α-to-N functionalization in 71% yield (Figure 3B). In complete accordance with the funding principles of the HAcTive strategy, the use of regioisomeric aldehyde **1e** redirected the selectivity toward the α-to-O position (57%, Figure 3B, see also Section 9 in the Supporting Information). Taken together, these findings suggested that the HAcTive strategy represents a streamlined approach for the versatile synthesis of amino alcohols.

After a quick round of optimization of reaction conditions (Section 5.1 in the Supporting Information), we reacted **1d** with a wide array of electron-poor olefins to forge C($sp^3$)–C($sp^3$) bonds (Figure 4). Starting from α,β-unsaturated ketones, the reaction occurred smoothly with methyl vinyl ketone and methylene norbornanone, allowing to obtain the expected adducts **14** and **15** in 66% and 76% yield after isolation, respectively. Next, we found that acrylates were elective compounds in the role of SOMOphiles (**16**-**23**), reliably producing the corresponding hydroalkylation products in high yields (50-83%). Intriguingly, complex acrylates derived from biologically relevant alcohols, such as prolinol, galactose, cholesterol and menthol, were also successfully employed (**20**-**23**, 50-83%), underscoring the robustness and applicability of this protocol. Olefins bearing other electron-withdrawing functional groups were also well tolerated (**24**-**27**, 65-79%). Radical addition onto 2-benzylidenemalononitrile proceeded well and resulted in the formation of adduct **25** in 79% yield (dr 1.2:1). Similarly, (vinylsulfonyl)benzene and 2-vinylpyridine allowed to prepare the corresponding Giese adducts **26** and **27** in satisfying yields (65% and 75%, respectively).

Motivated by these findings, we subsequently developed a protocol for the SOMOphilic alkynylation of the Garner's aldehyde (see Section 5.2 in the Supporting Information).[40,41] Although the expected products were generally not obtained in outstanding yields (Figure 4), it is important to stress that our approach offers a new metal-free retrosynthetic perspective for the synthesis of alkynyl amino alcohols (and amino acids), which are more traditionally obtained via a Sonogashira-type cross-coupling.[42]

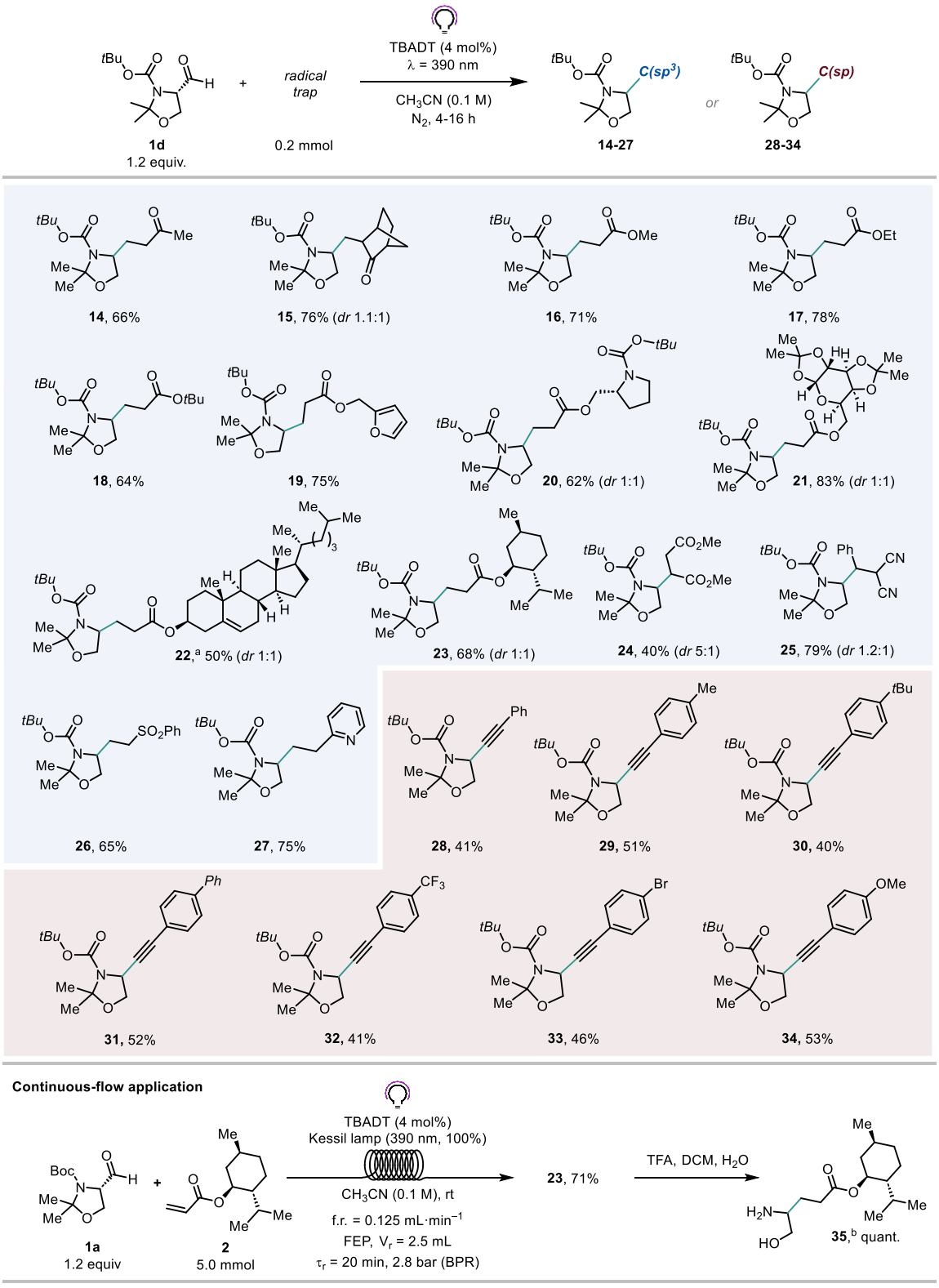


***Figure 4*** – Scope of the decarbonylative alkylation of the Garner's aldehyde (**1d**) for the formal synthesis of amino alcohols. All yields are meant after isolation. Reaction conditions for $C(sp^3)$–$C(sp^3)$ bond formation: **1d** (1.2 equiv.), olefin (0.2 mmol) and TBADT (4 mol%) in $CH_3CN$ (0.1 M). The reaction mixture was bubbled with $N_2$ (2 min) and irradiated at 390 nm for 16 h. Reaction conditions for $C(sp^3)$–$C(sp)$ bond formation: **1d** (1.2 equiv.), alkynyl sulfone (0.2 mmol) and TBADT (4 mol%) in $CH_3CN$ (0.1 M). The reaction mixture was bubbled with $N_2$ (2 min) and irradiated at 390 nm for 4 h. [a] Reaction performed in $CH_3CN/CH_2Cl_2$ (0.05 M). [b] Reaction performed on 0.2 mmol of **23**.

The α-to-O functionalization was never observed. Thus, several *para*-substituted ((methylsulfonyl)ethynyl)benzenes allowed to obtain the expected products **28**-**34** in moderate yields after isolation (40-53%).

In an attempt to reduce the reaction time and enable scalability of the protocol, we managed to translate the transformation into continuous flow for product **23** (Figure 4, lower part; see Sections 6.3 in the Supporting Information). Thus, a $CH_3CN$ solution of **1d**, menthyl acrylate and TBADT was pushed by means of a syringe pump into a photochemical reactor (FEP, $V_R$ = 2.5 mL, ID = 0.8 mm, see Figure S2). As expected, when the reaction was performed in the absence of a back-pressure regulator (BPR), the flow regime was irregular because of CO gas evolution and the residence time was not reproducible. The installation of a BPR (2.8 bar) at the outlet of the photochemical reactor solved this issue and allowed to obtain **23** in 71% yield on a 5 mmol scale. As expected, the oxazolidine ring could be opened in acidic conditions to unveil the corresponding α-to-N-functionalized amino alcohol **35** in quantitative yield.

Next, we shifted our focus to understanding the origin of selectivity of the HAT step by adopting a combined experimental and computational approach. On the one hand, we used Laser-Flash Photolysis (LFP) to appreciate the kinetic advantage offered by the HAcTive strategy. In more detail, we opted to measure the quenching rates of the excited state of TBADT (see Section 9.2 in the Supporting Information) by a set of *tagged* H-donors used in this work and compared them with those obtained by using the corresponding *untagged* scaffolds. In practice, we constructed the relevant Stern-Volmer (SV) plots and calculated the corresponding absolute kinetic constants for the HAT step. The kinetic data for substrates **S1** vs **1a** and **1d** vs **S4** are presented in Figure 5A (left), while additional substrate comparisons are shown in Figure 5A (right). In all cases, SV analysis consistently showed the kinetic advantage of using *tagged* substrates and, in some cases, quenching rates proved to be 5-10 times higher than those of *untagged* ones. Of note, the reported kinetic constants have not been corrected for the number of hydrogen atoms. These experiments strongly suggest that kinetics plays a fundamental role in the HAcTive strategy.

In parallel, we conducted DFT calculations at the ωB97xD/def2TZVP level of theory (implicit $CH_3CN$ solvent) to have insight into the reasons for the observed selectivity (see Section 9.3 in the Supporting Information for further details). In particular, we modelled H-abstraction from all the available positions in model compounds **1a** ($\mathbf{H_{a\text{-}c}}$) and untagged derivative **S1** ($\mathbf{H_{a,b}}$; see Figure 5B). As the hydrogen abstractor, we decided to adopt the *tert*-butoxyl radical (*t*BuO$^\bullet$) based on the assumption that most photocatalysts operating via direct HAT (when in the excited state) show a behaviour analogous to this alkoxyl radical.[43] Furthermore, *t*BuO$^\bullet$ is a convenient computational choice due to the limited computational cost and the symmetric substitution pattern of the *tert*-butyl group, that limits the number of conformations to be screened.

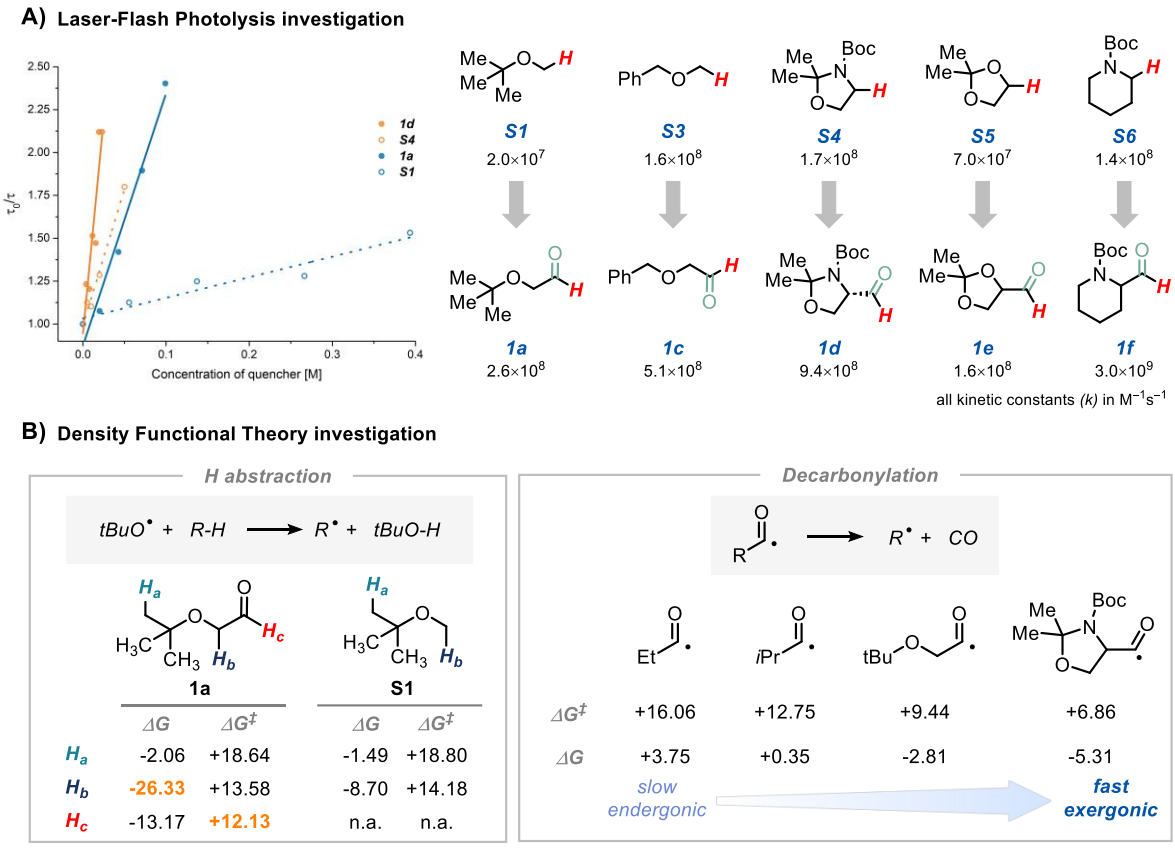


Figure 5 – Mechanistic studies: A) Laser-Flash Photolysis experiments and B) Density Functional Theory analysis.

Figure 5B (left) describes the thermodynamic (ΔG) and kinetic (ΔG‡) parameters associated with the hydrogen abstraction processes by the *tert*-butoxyl radical from the different positions of **1a** and **S1**. Importantly, ΔG values offer indications about both the relative strength of the cleaved C–H bonds and the relative stability of the generated C-centered radicals. On one hand, the introduction of the HAcTive group has a negligible impact on both thermodynamic and kinetic parameters of **H$_a$** (methyl position). On the other hand, the incorporation of the TAG has a tremendous impact on the lability of C–**H$_b$** bond (ΔΔG ≃ 18 kcal mol$^{-1}$) since in this case a highly stabilized captodative radical is formed upon cleavage of named bond. Furthermore, **1a** features an additional (quite) labile position, namely formyl C-**H$_c$**, with the overall bond dissociation energy (BDE) order for **1a**: C–**H$_a$** >> C–**H$_c$** > C–**H$_b$**, somehow contradicting the experimental selectivity toward the C–**H$_c$** position. In the context of radical chemistry, it is well-established that selectivity profiles often emerge from kinetic rather than thermodynamic factors.[34] Actually, the activation energy for C–H cleavage (ΔG‡) follows the order: C–**H$_a$** >> C–**H$_b$** > C–**H$_c$**. This behaviour can be rationalized based on polar effects governing the transition state for the C–H cleavage: it is no surprise that the electrophilic *tert*-butoxyl radical targets the most hydridic C–H site, namely the formyl one (C–**H$_c$**), with exquisite selectivity. Collectively, these results point towards kinetic selectivity too: although weaker bonds are present in *tagged* substrates, TAG is able to guide HAT.[44]

Another key aspect for the success of the HAcTive strategy is the decarbonylation step, which has to be fast, avoiding any competitive reactivity of the initially formed acyl radical. Figure 5B (right) analyzes the behaviour of a set of diverse acyl radicals. Thus, decarbonylation of the acyl radicals deriving from substrates **1a** and **1d** has to confront with modest barriers (+9.44 kcal·mol$^{-1}$ and +6.86 kcal·mol$^{-1}$, respectively) and are overall exergonic processes. For the sake of comparison, the same process has been modelled for the acyl radicals arising from propanaldehyde and isobutyraldehyde, taken as reference for primary and secondary acyl radicals, respectively. Thus, decarbonylation of the former is slightly endergonic ($\Delta G$ = +3.75 kcal·mol$^{-1}$) and kinetically challenging ($\Delta G^{\ddagger} \simeq$ +16 kcal·mol$^{-1}$). In contrast, the decarbonylation of the secondary acyl radical is almost thermoneutral and occurs with a smaller activation energy ($\Delta G^{\ddagger} \simeq$ +13 kcal·mol$^{-1}$) than the primary one. On one side, this analysis highlights an important aspect of the HAcTive strategy: its efficiency is closely linked to the decarbonylation step, making it particularly well-suited for generating stabilized carbon-centered radicals (e.g. α-to-heteroatom ones). On the other side, it suggests the formyl group as a « super » hydrogen donor, capable of guiding selectivity despite the presence of weaker C–H bonds within the substrates and boosting efficiency in the HAT step thanks to kinetic factors. Importantly, an additional advantage of the proposed approach is the traceless nature of the CO group, which does not leave residues to get rid of at the end of the process.

## CONCLUSION

We developed the HAcTive strategy, which harnesses kinetic factors inherent to the HAT step to tackle persistent challenges in photocatalyzed HAT, specifically regioselectivity and inefficiency. This approach involves exploiting the formyl group as a traceless activating group (TAG) at the targeted position on the substrate. The rapid HAT from the highly hydridic formyl C(sp$^2$)–H bond of aldehydes, followed by the α-fragmentation of the resulting acyl radical (i.e., decarbonylation), significantly enhances both regioselectivity and overall efficiency. A detailed experimental, spectroscopic and computational analysis validates the conceptual framework of the HAcTive strategy. We are confident that the results presented in this work will stimulate further research in the field of photocatalyzed HAT for the synthesis of pharmaceuticals and agrochemicals, as well as in the development of late-stage functionalization campaigns. Further studies are underway to further expand the strategy.

## ACKNOWLEDGEMENTS

This work has benefited from the equipment and framework of the COMP-HUB and COMP-R Initiatives, funded by the 'Departments of Excellence' programs of the Italian Ministry for University and Research (MUR, 2018–2027). We acknowledge support from UniPV and MUR through the program 'Departments of Excellence' (2023-2027). Financial support was provided by the Project PRIN PNRR 'LIGHT CAT'

(no. P2022RHMCM) supported by the European Commission – NextGeneration EU programme. VM was supported by National Programs (PON "Ricerca e Innovazione" 2014–2020 Azione IV.4 and Azione IV.5) of the Italian Ministry of University and Research (MUR). We acknowledge the CINECA award under the ISCRA initiative, for the availability of high-performance computing resources and support. NDC acknowledges PRIN2022 "COXSECAT" – (MUR, code:20223B4JWC). We also wish to thank Mattia Amariglio (UNIPR) and Prof. Alex Manicardi (UNIPR) for HPLC analyses and Dr. Paolo Ronchi (MCDDT, Chiesi Farmaceutici) for fruitful discussion.

## REFERENCES

1 Capaldo, L., Ravelli, D. & Fagnoni, M. Direct Photocatalyzed Hydrogen Atom Transfer (HAT) for Aliphatic C-H Bonds Elaboration. *Chem. Rev.* **122**, 1875-1924, doi:10.1021/acs.chemrev.1c00263 (2022).

2 Bonciolini, S., Noël, T. & Capaldo, L. Synthetic Applications of Photocatalyzed Halogen-Radical Mediated Hydrogen Atom Transfer for C–H Bond Functionalization. *Eur. J. Org. Chem.* **2022**, doi:10.1002/ejoc.202200417 (2022).

3 Ye, Z., Lin, Y. M. & Gong, L. The Merger of Photocatalyzed Hydrogen Atom Transfer with Transition Metal Catalysis for C–H Functionalization of Alkanes and Cycloalkanes. *Eur. J. Org. Chem.* **2021**, 5545-5556, doi:10.1002/ejoc.202101036 (2021).

4 Cao, H., Tang, X., Tang, H., Yuan, Y. & Wu, J. Photoinduced intermolecular hydrogen atom transfer reactions in organic synthesis. *Chem Catal.* **1**, 523-598, doi:10.1016/j.checat.2021.04.008 (2021).

5 Capaldo, L., Quadri, L. L. & Ravelli, D. Photocatalytic hydrogen atom transfer: the philosopher's stone for late-stage functionalization? *Green Chem.* **22**, 3376-3396, doi:10.1039/d0gc01035a (2020).

6 Ruffoni, A., Mykura, R. C., Bietti, M. & Leonori, D. The interplay of polar effects in controlling the selectivity of radical reactions. *Nat. Synth.* **1**, 682-695, doi:10.1038/s44160-022-00108-2 (2022).

7 Salamone, M. *et al.* Bimodal Evans-Polanyi Relationships in Hydrogen Atom Transfer from C(sp(3))-H Bonds to the Cumyloxyl Radical. A Combined Time-Resolved Kinetic and Computational Study. *J. Am. Chem. Soc.* **143**, 11759-11776, doi:10.1021/jacs.1c05566 (2021).

8 Milan, M., Salamone, M., Costas, M. & Bietti, M. The Quest for Selectivity in Hydrogen Atom Transfer Based Aliphatic C-H Bond Oxygenation. *Acc. Chem. Res.* **51**, 1984-1995, doi:10.1021/acs.accounts.8b00231 (2018).

9 Galeotti, M., Trasatti, C., Sisti, S., Salamone, M. & Bietti, M. Factors Governing Reactivity and Selectivity in Hydrogen Atom Transfer from C(sp(3))-H Bonds of Nitrogen-Containing Heterocycles to the Cumyloxyl Radical. *J. Org. Chem.* **87**, 7456-7463, doi:10.1021/acs.joc.2c00955 (2022).

10 Salamone, M., Carboni, G. & Bietti, M. Fine Control over Site and Substrate Selectivity in Hydrogen Atom Transfer-Based Functionalization of Aliphatic C-H Bonds. *J. Org. Chem.* **81**, 9269-9278, doi:10.1021/acs.joc.6b01842 (2016).

11 Salamone, M. & Bietti, M. Tuning reactivity and selectivity in hydrogen atom transfer from aliphatic C-H bonds to alkoxyl radicals: role of structural and medium effects. *Acc. Chem. Res.* **48**, 2895-2903, doi:10.1021/acs.accounts.5b00348 (2015).

12 Galeotti, M., Salamone, M. & Bietti, M. Electronic control over site-selectivity in hydrogen atom transfer (HAT) based C(sp(3))-H functionalization promoted by electrophilic reagents. *Chem. Soc. Rev.* **51**, 2171-2223, doi:10.1039/d1cs00556a (2022).

13 Cao, H. *et al*. Brønsted acid-enhanced direct hydrogen atom transfer photocatalysis for selective functionalization of unactivated C(sp3)–H bonds. *Nat*. *Synth*. **1**, 794-803, doi:10.1038/s44160-022-00125-1 (2022).
14 Shaw, M. H., Twilton, J. & MacMillan, D. W. Photoredox Catalysis in Organic Chemistry. *J*. *Org*. *Chem*. **81**, 6898-6926, doi:10.1021/acs.joc.6b01449 (2016).
15 McAtee, R. C., McClain, E. J. & Stephenson, C. R. J. Illuminating Photoredox Catalysis. *Trends Chem*. **1**, 111-125, doi:10.1016/j.trechm.2019.01.008 (2019).
16 Chan, A. Y. *et al*. Metallaphotoredox: The Merger of Photoredox and Transition Metal Catalysis. *Chem*. *Rev*. **122**, 1485-1542, doi:10.1021/acs.chemrev.1c00383 (2022).
17 Romero, N. A. & Nicewicz, D. A. Organic Photoredox Catalysis. *Chem*. *Rev*. **116**, 10075-10166, doi:10.1021/acs.chemrev.6b00057 (2016).
18 Stephenson, C., Yoon, T. & MacMillan, D. W. C. *Visible Light Photocatalysis in Organic Chemistry*. (2018).
19 Chatgilialoglu, C., Crich, D., Komatsu, M. & Ryu, I. Chemistry of Acyl Radicals. *Chem*. *Rev*. **99**, 1991-2070, doi:10.1021/cr9601425 (1999).
20 Cao, H. *et al*. Photoinduced site-selective alkenylation of alkanes and aldehydes with aryl alkenes. *Nat*. *Commun*. **11**, 1956, doi:10.1038/s41467-020-15878-6 (2020).
21 Wang, L. *et al*. Direct C–H Arylation of Aldehydes by Merging Photocatalyzed Hydrogen Atom Transfer with Palladium Catalysis. *ACS Catal*. **10**, 7543-7551, doi:10.1021/acscatal.0c02105 (2020).
22 Kuang, Y. *et al*. Asymmetric Synthesis of 1,4-Dicarbonyl Compounds from Aldehydes by Hydrogen Atom Transfer Photocatalysis and Chiral Lewis Acid Catalysis. *Angew*. *Chem*. *Int*. *Ed*. **131**, 17015-17019, doi:10.1002/ange.201910414 (2019).
23 Bonassi, F., Ravelli, D., Protti, S. & Fagnoni, M. Decatungstate Photocatalyzed Acylations and Alkylations in Flow via Hydrogen Atom Transfer. *Adv*. *Synth*. *Catal*. **357**, 3687-3695, doi:10.1002/adsc.201500483 (2015).
24 Ravelli, D., Zema, M., Mella, M., Fagnoni, M. & Albini, A. Benzoyl radicals from (hetero)aromatic aldehydes. Decatungstate photocatalyzed synthesis of substituted aromatic ketones. *Org*. *Biomol*. *Chem*. **8**, 4158-4164, doi:10.1039/c0ob00066c (2010).
25 Esposti, S., Dondi, D., Fagnoni, M. & Albini, A. Acylation of electrophilic olefins through decatungstate-photocatalyzed activation of aldehydes. *Angew*. *Chem*. *Int*. *Ed*. **46**, 2531-2534, doi:10.1002/anie.200604820 (2007).
26 Tzirakis, M. D. & Orfanopoulos, M. Acyl radical reactions in fullerene chemistry: direct acylation of [60]fullerene through an efficient decatungstate-photomediated approach. *J*. *Am*. *Chem*. *Soc*. **131**, 4063-4069, doi:10.1021/ja808658b (2009).
27 Liu, Y. L., Ouyang, Y. J., Zheng, H., Liu, H. & Wei, W. T. Recent advances in acyl radical enabled reactions between aldehydes and alkenes. *Chem*. *Commun*. **57**, 6111-6120, doi:10.1039/d1cc02112e (2021).
28 Fan, X. Z. *et al*. Eosin Y as a Direct Hydrogen-Atom Transfer Photocatalyst for the Functionalization of C-H Bonds. *Angew*. *Chem*. *Int*. *Ed*. **57**, 8514-8518, doi:10.1002/anie.201803220 (2018).
29 Capaldo, L., Ertl, M., Fagnoni, M., Knör, G. & Ravelli, D. Antimony–Oxo Porphyrins as Photocatalysts for Redox-Neutral C–H to C–C Bond Conversion. *ACS Catal*. **10**, 9057-9064, doi:10.1021/acscatal.0c02250 (2020).
30 Kuang, Y. *et al*. Asymmetric Synthesis of 1,4-Dicarbonyl Compounds from Aldehydes by Hydrogen Atom Transfer Photocatalysis and Chiral Lewis Acid Catalysis. *Angew*. *Chem*. *Int*. *Ed*. **58**, 16859-16863, doi:10.1002/anie.201910414 (2019).
31 Wang, X., Chen, Y., Song, H., Liu, Y. & Wang, Q. Synthesis of Unnatural α-Amino Acids via Photoinduced Decatungstate-Catalyzed Giese Reactions of Aldehydes. *Org*. *Lett*. **23**, 2199-2204, doi:10.1021/acs.orglett.1c00345 (2021).
32 Tzirakis, M. D., Lykakis, I. N. & Orfanopoulos, M. Decatungstate as an efficient photocatalyst in organic chemistry. *Chem*. *Soc*. *Rev*. **38**, 2609-2621, doi:10.1039/b812100c (2009).

33 Singh, P. P., Sinha, S., Gahtori, P., Tivari, S. & Srivastava, V. Recent advances of decatungstate photocatalyst in HAT process. *Org. Biomol. Chem.*, 2523-2538, doi:10.1039/d4ob00213j (2024).
34 Ravelli, D., Fagnoni, M., Fukuyama, T., Nishikawa, T. & Ryu, I. Site-Selective C–H Functionalization by Decatungstate Anion Photocatalysis: Synergistic Control by Polar and Steric Effects Expands the Reaction Scope. *ACS Catal.* **8**, 701-713, doi:10.1021/acscatal.7b03354 (2017).
35 Sun, J. *et al.* Simplified Modular Access to Enantiopure 1,2-Aminoalcohols via Ni-Electrocatalytic Decarboxylative Arylation. *J. Am. Chem. Soc.* **146**, 6209-6216, doi:10.1021/jacs.3c14119 (2024).
36 Laarhoven, L. J. J. & Mulder, P. α-C−H Bond Strengths in Tetralin and THF: Application of Competition Experiments in Photoacoustic Calorimetry. *The Journal of Physical Chemistry B* **101**, 73-77, doi:10.1021/jp960982n (1997).
37 Wayner, D. D. M., Clark, K. B., Rauk, A., Yu, D. & Armstrong, D. A. C−H Bond Dissociation Energies of Alkyl Amines: Radical Structures and Stabilization Energies. *J. Am. Chem. Soc.* **119**, 8925-8932, doi:10.1021/ja971365v (1997).
38 Passiniemi, M. & Koskinen, A. M. Garner's aldehyde as a versatile intermediate in the synthesis of enantiopure natural products. *Beilstein J. Org. Chem.* **9**, 2641-2659, doi:10.3762/bjoc.9.300 (2013).
39 Synthesis of 1,1-Dimethylethyl (S)-4-Formyl-2,2-Dimethyl-3-Oxazolidinecarboxylate by Oxidation of the Alcohol. *Organic Syntheses* **77**, doi:10.15227/orgsyn.077.0064 (2000).
40 Ge, D., Wang, X. & Chu, X.-Q. SOMOphilic alkynylation using acetylenic sulfones as functional reagents. *Org. Chem. Front.* **8**, 5145-5164, doi:10.1039/d1qo00798j (2021).
41 Capaldo, L. & Ravelli, D. Decatungstate as Direct Hydrogen Atom Transfer Photocatalyst for SOMOphilic Alkynylation. *Org. Lett.* **23**, 2243-2247, doi:10.1021/acs.orglett.1c00381 (2021).
42 Yamakawa, T. *et al.* Total synthesis of tryprostatins A and B. *Tetrahedron* **67**, 6547-6560, doi:10.1016/j.tet.2011.05.112 (2011).
43 Waele, V. D., Poizat, O., Fagnoni, M., Bagno, A. & Ravelli, D. Unraveling the Key Features of the Reactive State of Decatungstate Anion in Hydrogen Atom Transfer (HAT) Photocatalysis. *ACS Catal.* **6**, 7174-7182, doi:10.1021/acscatal.6b01984 (2016).
44 Garwood, J. J. A., Chen, A. D. & Nagib, D. A. Radical Polarity. *J. Am. Chem. Soc.*, doi:10.1021/jacs.4c06774 (2024).